Exceptional Points in a Microwave Billiard with Time-Reversal Invariance Violation

B. Dietz,[1] H. L. Harney,[2] O. N. Kirillov,[3] M. Miski-Oglu,[1] A. Richter,[1,4,*] and F. Schäfer[1,5]

[1]*Institut für Kernphysik, Technische Universität Darmstadt, D-64289 Darmstadt, Germany*
[2]*Max-Planck-Institut für Kernphysik, D-69029 Heidelberg, Germany*
[3]*FWSH, Helmholtz-Zentrum Dresden-Rossendorf, Post Office Box 510119, D-01314 Dresden, Germany*
[4]*ECT*, Villa Tambosi, I-38123 Villazzano (Trento), Italy*
[5]*LENS, University of Florence, I-50019 Sesto-Fiorentino (Firenze), Italy*

(Received 13 August 2010; published 15 April 2011)

We report on the experimental study of an exceptional point (EP) in a dissipative microwave billiard with induced time-reversal invariance ($\mathcal{T}$) violation. The associated two-state Hamiltonian is non-Hermitian and nonsymmetric. It is determined experimentally on a narrow grid in a parameter plane around the EP. At the EP the size of $\mathcal{T}$ violation is given by the relative phase of the eigenvector components. The eigenvectors are adiabatically transported around the EP, whereupon they gather geometric phases and in addition geometric amplitudes different from unity.

DOI: 10.1103/PhysRevLett.106.150403 PACS numbers: 03.65.Vf, 02.10.Yn, 05.45.Mt, 11.30.Er

We present experimental studies of two nearly degenerate eigenmodes in a dissipative microwave cavity with induced $\mathcal{T}$ violation. The Hamiltonian is not Hermitian [1–4] and thus may possess an exceptional point (EP), where two or more eigenvalues and also the associated eigenvectors coalesce. In contrast, at a degeneracy of a Hermitian Hamiltonian, a so-called diabolical point (DP), the eigenvectors are linearly independent [5,6]. The occurrence of EPs [2,7] in the spectrum of a dissipative system was studied in quantum physics [8] as well as in classical physics [9]. The first experimental evidence of EPs came from flat microwave cavities [10–13], which are analogues of quantum billiards [14]. Subsequently EPs were observed in coupled electronic circuits [15] and recently in chaotic microcavities and atom-cavity quantum composites [16]. The present contribution is the first experimental study of an EP under $\mathcal{T}$ violation. It is induced via magnetization of a ferrite inside the cavity by an external field B [17]. $\mathcal{T}$ violation caused by B is commonly distinguished from dissipation [18]. For a nondissipative system with broken $\mathcal{T}$ invariance ($B \neq 0$) the Hamiltonian is Hermitian. For a dissipative system the energy is not conserved such that for $B = 0$ it is described by a complex symmetric Hamiltonian. This case is referred to as the $\mathcal{T}$-invariant one [18].

To realize a coalescence of a doublet of eigenmodes in the experiment two parameters are varied. Since the doublets are well separated from neighboring resonances, the effective Hamiltonian is two-dimensional. Its four complex elements are determined on a narrow grid in the parameter plane, thus yielding an unprecedented set of data. This allows us (i) to quantify the size of $\mathcal{T}$ violation and (ii) to measure to a high precision the geometric phase [5,6] and the geometric amplitude [1,19,20] that the eigenvectors gather when encircling an EP. An earlier rule [11] is generalized to the case of $\mathcal{T}$ violation [1].

The setup is similar to that used in [11,12]. The resonator is constructed from three 5 mm thick copper plates, which are sandwiched on top of each other. The center plate has a hole with the shape of two half circles of 250 mm in diameter, which are separated by a 10 mm bar of copper except for an opening of 80 mm length (see the inset of Fig. 1). The opening allows a coupling of the electric field modes excited in each half circle, which is varied with a movable gate of copper of length 80 mm and width 3 mm inserted through a small slit in the top plate and operated by a micrometer stepper motor. The bottom of this gate is tilted for a precise setting of the coupling. When closing the gate it eventually plunges into a notch in the bottom plate. Its lifting s defines one parameter with

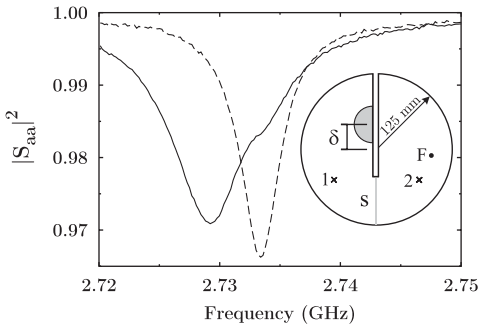

FIG. 1. Spectra measured at antenna 1 (solid) and 2 (dashed) for $s = 1.66$ mm, $\delta = 41.50$ mm, $B = 53$ mT. We observe a single resonance at antenna 2, and a much broader one with a shoulder at the peak position of the former at antenna 1. Thus one eigenmode is localized in the right part of the cavity, whereas the second one penetrates from the left into the right one. Inset: top view (to scale) of the microwave cavity. Both halves are connected via an opening of size s (gray bar). A semicircular Teflon disk (gray) is put at a distance δ from the center, a ferrite at F.

0 mm (no coupling) $\leq s \leq$ 9 mm (full coupling). The left half of the cavity in Fig. 1 contains a movable semicircular Teflon piece with diameter 60 mm and height 5 mm connected via a thin snell to another stepper motor. Its displacement with respect to the center of the cavity defines the other parameter δ.

A pointlike dipole antenna intrudes into each half of the cavity. A vectorial network analyzer Agilent PNA 5230 A couples microwaves into the cavity through one antenna a and measures amplitude and phase of the signal received at the same or the other antenna b relative to the input signal. In this way the complex element S_{ba} of the scattering matrix S is determined. To induce $\mathcal{T}$ violation, a cylindrical ferrite of diameter 4 mm and height 5 mm [17] is put in the right part of the cavity and magnetized by two permanent magnets, which are mounted above and below the cavity. Magnetic field strengths 0 mT $\leq B \leq$ 90 mT are obtained by varying their distance. To scan the parameter space spanned by (s, δ), the two stepper motors and the vectorial network analyzer are controlled by a PC. The four S-matrix elements $S_{ba}(f)$, $\{a, b\} \in \{1, 2\}$ are measured in the parameter plane with the resolution $\Delta s = \Delta\delta = 0.01$ mm and a frequency step $\Delta f = 10$ kHz. The frequency range of 40 MHz is determined by the spread of the resonance doublet. Lack of reciprocity, i.e., $S_{12} \neq S_{21}$, is the signature for $\mathcal{T}$ violation [17]. Figure 1 shows two typical spectra for $|S_{aa}|^2$ with $a = 1, 2$. Additional measurements include neighboring resonances, situated about 250 MHz away from the region of interest, to account for their residual influence. In the considered frequency range the electric field vector is perpendicular to the top and bottom plates. Then, the Helmholtz equation is identical to the Schrödinger equation for the corresponding quantum billiard [14,21]. Consequently, the results provide insight into the associated quantum problem. In previous experiments [11,12] an EP was located by determining for each parameter setting the real and imaginary parts of the eigenvalues as the frequencies $f_{1,2}$ and the widths $\Gamma_{1,2}$ of the resonances from a fit of a Breit-Wigner function. This procedure, however, fails at the EP because there the line shape is not a first order pole of the S matrix but rather the sum of a first and a second order pole [4,13]. Therefore, the coalescence of the eigenvectors should also be incorporated [12,13]. We determine the two-state Hamiltonian H and its eigenvalues and eigenvectors explicitly for every setting of s, δ, B from the measured S-matrix elements via the method presented in [17]. There, we showed that for two pointlike antennas a resonance doublet is well described by the two-channel S matrix $S(f) = \mathbf{1} - 2\pi i W^\dagger (f\mathbf{1} - H)^{-1} W$. The matrix $W = (W_{\mu a})$ couples the resonant states $\mu = 1, 2$ to the antennas $a = 1, 2$. It is real since that coupling conserves $\mathcal{T}$. The Hamiltonian H comprises dissipation in the resonator walls and the ferrite, and $\mathcal{T}$ violation and thus is neither Hermitian nor symmetric. Its general form reads

$$H = \begin{pmatrix} e_1 & H_{12}^S - iH_{12}^A \\ H_{12}^S + iH_{12}^A & e_2 \end{pmatrix}. \quad (1)$$

The quantities $e_1 \pm e_2$, H_{12}^S, and H_{12}^A are complex expansion coefficients with respect to the unit and the Pauli matrices. The ansatz for S was tested thoroughly by fitting it to S-matrix elements measured with and without magnetization of the ferrite. In the latter case the antisymmetric part H_{12}^A vanishes [11,12]. Fitting the S matrix to the four measured excitation functions $S_{ba}(f)$ yields the matrices H and W up to common real orthogonal basis transformations. We define the basis such that $(H_{12}^S + iH_{12}^A)/(H_{12}^S - iH_{12}^A) = \exp(2i\tau)$ is a phase factor. Thus, $\mathcal{T}$ violation is expressed by a real phase τ. This is the usual practice in physics, e.g., for nuclear reactions [22], and for weak and electromagnetic decay [23].

The eigenvalues of H in Eq. (1) coalesce to an EP when $H_{12}^{S^2} + H_{12}^{A^2} + (e_1 - e_2)^2/4 = 0$ but not all three terms vanish. Figure 2 shows one example for a search of the EP. Keeping $s = 1.66$ mm and $B = 53$ mT fixed, the real and imaginary parts of the eigenvalues, f_j and Γ_j, are plotted vs δ. At $(s_{\mathrm{EP}}, \delta_{\mathrm{EP}}) = (1.66 \pm 0.01, 41.25 \pm 0.01)$ mm the encounter of the eigenvalues is closest. To find the δ value for the coalescence of the eigenvectors $|r_k\rangle$, $k = 1, 2$, the ratios $\nu_k = r_{k1}/r_{k2} = |\nu_k| e^{i\Phi_k}$ of their components are determined [6]. The right part of Fig. 2 demonstrates that it also equals $\delta_{\mathrm{EP}} = 41.25$ mm. Indeed, as will be evidenced in further tests below, both the eigenvalues and the eigenvectors cross at $(s_{\mathrm{EP}}, \delta_{\mathrm{EP}})$. At the EP the only eigenvector of H is [3]

$$|r_{\mathrm{EP}}\rangle = \begin{pmatrix} ie^{i\tau} \\ 1 \end{pmatrix}. \quad (2)$$

The ratio of its components is a phase factor. For $\mathcal{T}$-conserving systems the phase is $\Phi_{\mathrm{EP}} = \pi/2$ [12] as confirmed by Fig. 3 at $B = 0$. With $\mathcal{T}$ violation $\Phi_{\mathrm{EP}} = \tau + \pi/2$ and thus provides a measure for τ. Figure 3 shows that τ goes through a maximum with increasing B. We identify this with the ferromagnetic resonance resulting

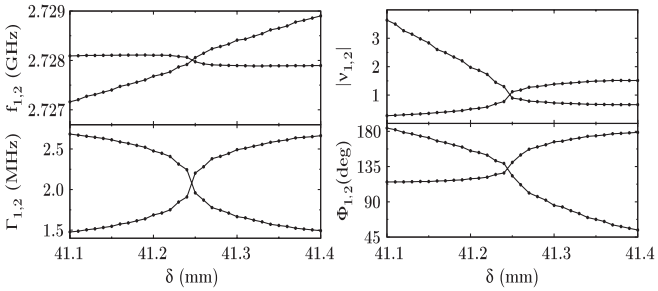

FIG. 2. Left panels: Real and imaginary parts of the eigenvalues, $f_{1,2}$ and $\Gamma_{1,2}$, as functions of δ at $s = s_{\mathrm{EP}} = 1.66$ mm and $B = 53$ mT. Around $\delta = \delta_{\mathrm{EP}} = 41.25$ mm they are closest. Right panels: Modulus and phase of the ratios $\nu_{1,2} = |\nu_{1,2}| e^{i\Phi_{1,2}}$ of the components of the associated eigenvectors. They are also closest at $\delta \simeq 41.25$ mm. For $\delta \leq \delta_{\mathrm{EP}}$ the upper curves correspond to, respectively, $f_1, \Gamma_1, |\nu_2|, \Phi_2$.

from the coupling of the rf magnetic field to the spins in the ferrite. In Ref. [17] the $\mathcal{T}$-violating matrix element iH_{12}^A has been expressed by a resonance formula which yields the solid curve for $\Phi_{EP}(B)$.

Figure 4(a) shows at $B = 53$ mT around an EP the differences of the complex eigenvalues, $f_{1,2}$ (blue, left of EP) and $\Gamma_{1,2}$ (orange, right of EP); 4(b) those of the phases $\Phi_{1,2}$ (orange, left of EP) and of the moduli $|\nu_{1,2}|$ (green, right of EP). The darker the color the smaller is the respective difference. The darkest color visualizes the branch cut along which it vanishes. The panels of Fig. 2 are cuts through the respective ones of Fig. 4 at $s = 1.66$ mm. We observe that $|f_1 - f_2|$ and $|\Phi_1 - \Phi_2|$ are small and thus visible only to the left of the EP, $|\Gamma_1 - \Gamma_2|$ and $||\nu_1| - |\nu_2||$ to its right. That the branch cuts all extend from one common point into opposite directions proves that this is an EP [2,6,16].

For systems with $\mathcal{T}$ violation the geometric phase γ gathered by the eigenvectors around an EP is predicted to be complex, yielding a geometric amplitude $e^{-\mathrm{Im}\gamma} \neq 1$ [1]. To check this we choose contours around the EP for the six values of B considered in Fig. 3. One example is shown in Fig. 4. It consists of two different loops [20]. The path is parametrized by a real variable t with initial value $t = 0$ at their intersection. After the first encircling $t = t_1$; after the second $t = t_2$. In [11,24] the geometric phase gathered around a diabolical point, respectively, an EP, was obtained for just a few parameter settings, because the procedure—the measurement of the electric field intensity distribution—is very time consuming. We now have the possibility to determine the left and right eigenvectors, $\langle l_j(t)|$ and $|r_j(t)\rangle$, $j = 1, 2$ of H in Eq. (1) on a much narrower grid of the parameter plane. In distinction to previous numerical works they are biorthonormalized at each point t of the contour such that $\langle l_j(t)|r_j(t)\rangle = 1$. Defining in analogy to the $\mathcal{T}$-conserving case [11] $\mathcal{B} = \frac{(e_1-e_2)}{2}/\sqrt{H_{12}^{S2} + H_{12}^{A2}}$, $\tan\theta = \sqrt{1+\mathcal{B}^2} - \mathcal{B}$ yields for the right eigenvectors [1]

$$|r_1(t)\rangle = \begin{pmatrix} e^{-i\tau/2}\cos\theta \\ e^{i\tau/2}\sin\theta \end{pmatrix}, \qquad |r_2(t)\rangle = \begin{pmatrix} -e^{-i\tau/2}\sin\theta \\ e^{i\tau/2}\cos\theta \end{pmatrix}. \tag{3}$$

As in [11] the EPs are located at $1 + \mathcal{B}^2 = 0$ and encircling the EP once changes θ to $\theta \pm \pi/2$. The $\mathcal{T}$-violating parameter τ is not constant along the contour, even though the magnetic field is fixed. In fact, it varies with the opening s between both parts of the resonator, because the ferrite is positioned in one of them (see Fig. 1). The position of the EP does not depend on τ. Thus, the space curve $(s(t), \delta(t), \tau(t))$ winds around the line $(s_{EP}, \delta_{EP}, \tau)$ (see Ref. [19]). Since τ has no singular points in the considered parameter plane it returns to its initial value after each encircling of the EP and the eigenvectors $|r_{1,2}(t)\rangle$ follow the same transformation scheme as in the $\mathcal{T}$-conserving case [11], that is, $|r_1(t_1)\rangle = |r_2(0)\rangle$, $|r_2(t_1)\rangle = -|r_1(0)\rangle$, and $|r_{1,2}(t_2)\rangle = -|r_{1,2}(0)\rangle$.

The biorthonormality defines the eigenvectors $\langle l_j|$ and $|r_j\rangle$ up to a geometric factor, so that $\langle L_j(t)| = \langle l_j(t)|e^{-i\gamma_j(t)}$ and $|R_j(t)\rangle = |r_j(t)\rangle e^{i\gamma_j(t)}$. The geometric phases $\gamma_j(t)$ are fixed by the condition of parallel transport [1,5], $\langle L_j(t)|\frac{d}{dt}R_j(t)\rangle = 0$. This yields $\frac{d\gamma_1(t)}{dt} = \frac{1}{2}\cos 2\theta(t)\frac{d\tau(t)}{dt} = -\frac{d\gamma_2(t)}{dt}$. The initial value of the phases is chosen as $\gamma_j(0) = 0$, such that $\gamma_1(t) = -\gamma_2(t)$. For the $\mathcal{T}$-conserving case $\gamma_{1,2}(t) \equiv 0$. The phase $\gamma_1(t)$ is determined successively for increasing t from the product of $\langle l_1(t)|$ and $|\frac{d}{dt}r_1(t)\rangle$. In the lower (upper) panel of Fig. 5 is plotted the phase $\gamma_1(t)$ accumulated by $|R_1(t)\rangle$ when encircling twice the EP along the contour in Fig. 4 (along its outer loop). The orientation is such that the EP is always to the left. The cusps occur at $\frac{d\tau}{dt} = 0$. In each panel the triangle marks the start point, the pentagon t_1, and the diamond t_2. In both examples $\gamma_1(t_1) \neq 0$ and, as predicted in Ref. [1], the geometric phase $\gamma_1(t_1)$ is not real. If the EP is encircled twice along the same loop, we obtain $\gamma_1(t_2) = 0$ [19,20] within 10^{-7}. Thus we measured the

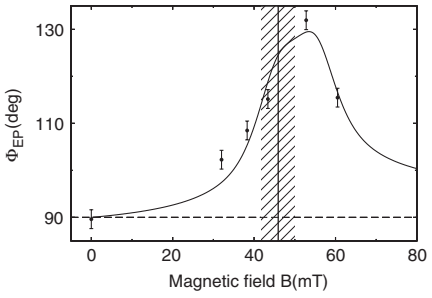

FIG. 3. Phase (dots) of the ratio ν_{EP} of the eigenvector components at the EP as a function of the magnetization of the ferrite. For the $\mathcal{T}$-conserving case the known result [12] of 90° (dashed horizontal line) is recovered. The model for the $\mathcal{T}$-violating matrix element iH_{12}^A in terms of the ferromagnetic resonance yields the solid line. The vertical bar indicates the range of B where the ferromagnetic resonance is expected.

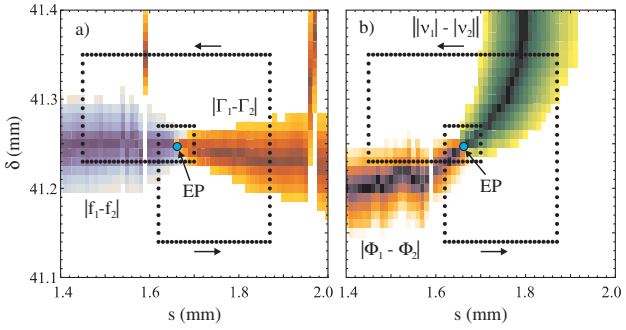

FIG. 4 (color). Differences of the complex eigenvalues $f_{1,2} + i\Gamma_{1,2}$ (a) and of the ratios $\nu_{1,2} = |\nu_{1,2}|e^{i\Phi_{1,2}}$ of the eigenvector components (b) in an area of the parameter plane (s, δ) around the EP. The darker the color the smaller is the respective difference. The black dots in both panels indicate the chosen contour for the encircling of the EP (see text).

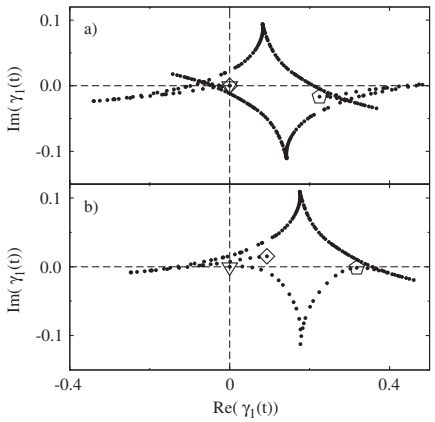

FIG. 5. The complex phase $\gamma_1(t)$ for $B = 53$ mT when encircling twice the EP along the contour shown in Fig. 4 (lower panel) or along its outer loop (upper panel). The triangle marks the start point, the pentagon t_1 after encircling the EP once, the diamond t_2 after a second encircling. There, $\gamma_1(t_2)$ equals $(3.123 - i3.474) \cdot 10^{-7}$; i.e., it is close to zero in the upper case, $0.0931 + i0.0152$ in the lower one.

γ's up to an accuracy manifestly better than 10^{-2}. Accordingly, from the value of $\gamma_1(t_2)$ given in the caption of Fig. 5, we may conclude that, when the loops are different, $\gamma_1(t)$ does not return to its initial value [20]. When encircling this double loop again and again we observe a drift of $\gamma_{1,2}$ in the complex plane away from the origin. Thus, one geometric amplitude increases and the other one decreases, yielding the experimental proof for the predicted reversible geometric pumping process [1]. The dependence on the choice of the path signifies that the complex phases $\gamma_{1,2}(t)$ are geometric and not topological. In order to obtain the complete phase gathered by $|R_1(t)\rangle$ during the encircling of the EP, one has to add the topological phase accumulated by $|r_1(t)\rangle$. In summary, when encircling the EP we obtain geometric factors different from unity and the transformation scheme Eq. (3) for $|\vec{r}_{1,2}(t)\rangle$. These results provide an unambiguous proof that the EP lies inside both loops of the contour shown in Fig. 4. Their precision is illustrated by the dense sequence of points in Fig. 5. It allows the determination of the size of $\mathcal{T}$ violation and of the geometric factor along arbitrary contours in the parameter plane. Predictions on geometric amplitudes and phases could be confirmed.

We thank G. Ripka and H. A. Weidenmüller for illuminating discussions. This work was supported by the DFG through SFB 634 and by the Alexander von Humboldt Foundation.

*richter@ikp.tu-darmstadt.de

[1] J. C. Garrison and E. M. Wright, Phys. Lett. A **128**, 177 (1988); M. V. Berry, Proc. R. Soc. A **430**, 405 (1990); K. Yu. Bliokh, J. Phys. A **32**, 2551 (1999).

[2] N. Moiseyev and S. Friedland, Phys. Rev. A **22**, 618 (1980); W. D. Heiss and A. L. Sannino, J. Phys. A **23**, 1167 (1990); E. Hernandez, A. Jauregui, and A. Mondragon, J. Phys. A **33**, 4507 (2000); A. P. Seyranian, O. N. Kirillov, and A. A. Mailybaev, J. Phys. A **38**, 1723 (2005).

[3] H. L. Harney and W. D. Heiss, Eur. Phys. J. D **29**, 429 (2004); W. D. Heiss, J. Phys. A **39**, 10 077 (2006).

[4] I. Rotter, J. Phys. A **42**, 153 001 (2009).

[5] M. V. Berry, Proc. R. Soc. A **392**, 45 (1984).

[6] M. V. Berry and M. R. Dennis, Proc. R. Soc. A **459**, 1261 (2003).

[7] T. Kato, *Perturbation Theory for Linear Operators* (Springer, Berlin, 1966).

[8] O. Latinne *et al.*, Phys. Rev. Lett. **74**, 46 (1995); E. Narevicius and N. Moiseyev, Phys. Rev. Lett. **84**, 1681 (2000); H. A. Weidenmüller, Phys. Rev. B **68**, 125326 (2003); H. Cartarius, J. Main, and G. Wunner, Phys. Rev. Lett. **99**, 173003 (2007); P. Cejnar, S. Heinze, and M. Macek, Phys. Rev. Lett. **99**, 100601 (2007); R. Lefebvre, O. Atabek, M. Sindelka, and N. Moiseyev, Phys. Rev. Lett. **103**, 123003 (2009); R. Lefebvre and O. Atabek, Eur. Phys. J. D **56**, 317 (2009).

[9] J. Wiersig, S. W. Kim, and M. Hentschel, Phys. Rev. A **78**, 053809 (2008); J.-W. Ryu, S.-Y. Lee, and S. W. Kim, Phys. Rev. A **79**, 053858 (2009); A. C. Or, Q. J. Mech. Appl. Math. **44**, 559 (1991); M. Kammerer, F. Merz, and F. Jenko, Phys. Plasmas **15**, 052 102 (2008); O. N. Kirillov, Proc. R. Soc. A **464**, 2321 (2008); S. Klaiman, U. Günther, and N. Moiseyev, Phys. Rev. Lett. **101**, 080402 (2008); Ch. E. Ruter *et al.*, Nature Phys. **6**, 192 (2010).

[10] M. Philipp, P. von Brentano, G. Pascovici, and A. Richter, Phys. Rev. E **62**, 1922 (2000).

[11] C. Dembowski *et al.*, Phys. Rev. Lett. **86**, 787 (2001); Phys. Rev. E **69**, 056216 (2004).

[12] C. Dembowski *et al.*, Phys. Rev. Lett. **90**, 034101 (2003).

[13] B. Dietz *et al.*, Phys. Rev. E **75**, 027201 (2007).

[14] H.-J. Stöckmann and J. Stein, Phys. Rev. Lett. **64**, 2215 (1990); H.-D. Gräf *et al.*, Phys. Rev. Lett. **69**, 1296 (1992).

[15] T. Stehmann, W. D. Heiss, and F. G. Scholtz, J. Phys. A **37**, 7813 (2004).

[16] S.-B. Lee *et al.*, Phys. Rev. Lett. **103**, 134101 (2009); Y. Choi *et al.*, Phys. Rev. Lett. **104**, 153601 (2010).

[17] B. Dietz *et al.*, Phys. Rev. Lett. **98**, 074103 (2007).

[18] F. Haake, *Quantum Signatures of Chaos* (Springer, New York, 2001).

[19] A. A. Mailybaev, O. N. Kirillov, and A. P. Seyranian, Phys. Rev. A **72**, 014104 (2005); Dokl. Math. **73**, 129 (2006).

[20] H. Mehri-Dehnavi and A. Mostafazadeh, J. Math. Phys. (N.Y.) **49**, 082 105 (2008).

[21] S. Sridhar, Phys. Rev. Lett. **67**, 785 (1991); A. Richter, in *Emerging Applications of Number Theory*, edited by D. A. Hejhal *et al.*, IMA Vol. 109 (Springer, New York, 1999), p. 479; H.-J. Stöckmann, *Quantum Chaos: An Introduction* (Cambridge University Press, Cambridge, 2000).

[22] H. Driller *et al.*, Nucl. Phys. **A317**, 300 (1979); J. M. Pearson and A. Richter, Phys. Lett. **56B**, 112 (1975).

[23] A. Richter, in *Interaction Studies in Nuclei*, edited by H. Jochim and B. Ziegler (North-Holland, Amsterdam 1975), p. 191.

[24] H.-M. Lauber, P. Weidenhammer, and D. Dubbers, Phys. Rev. Lett. **72**, 1004 (1994).